Vol. 23, n.°2, pp. 159-166, 2024
Revista UIS Ingenierías
https://revistas.uis.edu.co/index.php/revistauisingenierias

Quantized magnetic flux in a two-band superconducting condensate with a type-Kagome pinning center lattice

Flujo magnético cuantizado en un condensado superconductordes dos-bandas con centros de anclaje tipo red de Kagome

Cristhian Andres Aguirre [1, 2], Pablo Diaz [3], Jose Jose Barba-Ortega[4, 5]

[1] Departamento de Fiśica, Universidade Federal de Mato-Grosso, Cuiabá, Brasil. Orcid: 0000-0001-8064-6351.
Email: cristian@fisica.ufmt.br
[2] Departamento de Ciencias, Universidad ESEIT, Bogotá, Colombia.
[3] Departamento de Fiśica, Universidad de La Frontera, Temuco, Chile. Email: pablo.diaz@ufrontera.cl
[4] Departamento de Física, Universidad Nacional de Colombia, Bogotá, Colombia. Orcid: 0000-0003-3415-1811.
Email: jjbarbao@unal.edu.co
[5] Foundation of Researchers in Science and Technology of Materials, Bucaramanga, Colombia.

Received: 11 January 2024. Accepted: 23 March 2024. Final version: 3 June 2024.

Abstract

In this work we studied the vortex-configuration in a mesoscopic superconducting square in presence of an external magnetic field *H* applied parallel to its surface vector. We study the magnetization curves in a complete loop, the magnretic induction and the superconducting-electron density for the sample considering Neumann boundary conditions for the order parameter, via length Gennes extrapolation ($b \to \infty$). The sample presents a pinnin center as a Kagome-type laticce at different critical temperature. We solve the generalized time-dependent Ginzburg-Landau equations for a two-condensate system using the Link-variable method considering a *Field-Cooling* process. Our results show that the vortices are always located at the pinning centers in non-conventional configurations, due to cuopling used.

Keywords: Ginzburg-Landau; Superconductor; Type-II; Shubnikov-state; Vortices; Kagome lattice.

Resumen

En este trabajo estudiamos la configuración del vórtice en un cuadrado superconductor mesoscópico en presencia de un campo magnético externo *H* aplicado paralelo a su vector de superficie. Estudiamos las curvas de magnetización en bucle completo, la inducción magnética y la densidad de electrones superconductores para la muestra considerando las condiciones de contorno de Neumann para el parámetro de orden, mediante extrapolación de longitud de Gennes ($b \to \infty$). La muestra presenta un centro de anclaje tipo red de Kagome a diferente temperatura crítica. Resolvemos las ecuaciones generalizadas de Ginzburg-Landau dependientes del tiempo para un sistema de dos condensados usando el método de variable de enlace considerando un proceso *enfriamiento de campo*. Nuestros resultados muestran que los vórtices siempre están ubicados en los centros de anclaje con configuraciones no convencionales, debido al acoplamiento utilizado.

ISSN Online: 2145 - 8456

How to cite: C. A. Aguirre, P. Diaz, J. Barba-Ortega, “Quantized magnetic flux in a two-band superconducting condensate with a type-Kagome pinning center lattice,” *Rev. UIS Ing.*, vol. 23, no. 2, pp. 159-166, 2024, doi: https://doi.org/10.18273/revuin.v23n2-2024010

Palabras clave: Ginzburg-Landau; Superconductor; Type-II; Shubnikov-state; Vortices; Kagome lattice.

1. Introduction

A superconductor is a material that can conduct electricity without resistance, meaning that it can transmit electrical current indefinitely without any loss of energy. Superconductors are characterized by a critical temperature T_c below which they exhibit superconductivity. Two-condensates superconductivity, also known as two-band superconductivity, is a phenomenon that occurs in some materials where there are two different types of electrons or condensates that contribute to the superconductivity. These two-condensates can have different T_c, allowing the material to exhibit superconductivity at higher temperatures than a single-band superconductor. Two-condensates can interact with each other, leading to interesting phenomena such as a re-entrant superconducting phase diagram, where the material goes through multiple superconducting phases as the temperature or magnetic field is varied. This type of superconductivity has been observed in several materials (MgB_2, whit $T_c \sim 39K$ and iron-based superconductors, with $T_c \sim 55K$) and has been widely studied theoretically using computational methods [1], [2], [3], [4], [5], [6], [7], [9], [10].

The study of two-condensate superconductivity is an active area of research in condensed matter physics, with potential applications in high-temperature superconductivity and quantum computing, for this is important to control the vortex state by pinning centers, for example, including structural o topological defects into the sample. A good candidate for this is, the kagome-lattice structure, this lattice consisting of interconnected triangles arranged in a hexagonal pattern [11], [12], [13], [14]. Some materials with Kagome-lattice structures, such as iron-based superconductors and ruthenate-based superconductors, have also been studied extensively in recent years. These studies have revealed that the superconductivity in these materials is closely related to the electronic properties of the Kagome-lattice structure. Overall, the study of Kagome-lattice structures in superconductors is a promising field that could lead to the discovery of new materials with high-temperature superconductivity and other exotic electronic properties [15], [16], [17], [18], [19].

Several theoretical and experimental works have been carried out in this area, for example, F. Du et al., studied the interplay of superconductivity with electronic and structural instabilities on the Kagome lattice in vanadium-based kagome metals AV_3Sb_5 founding that this material exhibit superconductivity on an almost ideal kagome lattice, with the superconducting transition temperature forming two domes upon pressure tuning and that distortions of the crystal structure modulate superconductivity in this sample under pressure, providing a platform to study kagome lattice superconductivity in the presence of multiple electronic and structural instabilities [20]. S. Gazit et al., described a theoretical model for a Kagome lattice two-band superconductor and the emergent Dirac fermions and broken symmetries that arise in the confined and deconfined phases [21]. T. Neuper et al., showed that the lattice geometry, topological electron of the compounds KV_3Sb_5, CsV_3Sb_5 and RbV_3Sb_5, play a role in determining the properties of materials with a Kagome lattice structure and exhibit superconductivity at low temperature and an unusual charge order at high temperature, revealing a connection to the underlying topological nature of the band structure [22]. K. Jiang et al., reported progress on the experimental and theoretical studies of AV_3Sb_5 with (A=K,Rb,Cs), as an unconventional kagome superconducting sample. They found several theoretical models about the nature of the time-reversal symmetry breaking [23]. J. S. Leon et al., studied theoretically using the Ginburg-Landau model, the magnetization and the vortex state in a mesoscopic superconducting sample with a Honeycomb and Kagome structure in regions with suppressed superconductivity, they found that is possible to control the magnetic response of the sample and to manipulate the vortex configuration whit this kind of topological defects [24]. Rui Lou et al. studied the electronic properties of the charge density wave (CDW) and superconductivity in Kagome metal and observed the superconducting gap on both the electron band and the flat band around implying the multi-band superconductivity and offering insights into the relationship between CDW and superconductivity [25]. This paper is outlined as follows. In Section 2 we describe the theoretical formalism used to study a superconducting sample. In Section 3 we present the results and finally, in Section 4 we present our conclusions.

2. Theoretical Formalism

In this present work, we will study the superconducting matter in a two-condensate thin square of size $L = 30\xi_{10}$ with a Kagome lattice of circular defects of radius $r = \xi_{10}$ in presence of an external applied magnetics field H (see Figure 1). We will consider the Gibbs functional $\mathcal{G}(\psi_i, \mathbf{A})$ for a two-condensate with a Josephson-coupling $\Xi(\psi_1, \psi_2)$, where ψ_1 is the superconducting order parameter complex pseudo-function $\psi_i = |\psi_i| e^{i\theta_i}$, ($\theta_i$ its phase) for the i=1, 2 condensate, $\mathbf{A}$ is the magnetic

potential related to magnetic induction as $\mathbf{B} = \nabla \times \mathbf{A}$ [7], [8]:

$$\mathcal{G} = \int dV \left(\sum_{i}^{2} \mathcal{F}(\psi_i, \boldsymbol{A}) + \frac{1}{8\pi} |\mathbf{B}|^2 + \Xi(\psi_i) \right) \quad (1)$$

with:

$$F = \alpha_i |\psi_i|^2 + \frac{\beta_i}{2} |\psi_i|^4 + \frac{\zeta_i}{2m_i} |(i\hbar\nabla + 2e\mathbf{A})\psi_i|^2 \quad (2)$$

and

$$\Xi(\psi_1, \psi_2) = \gamma(\psi_1^* \psi_2 + \psi_2^* \psi_1). \quad (3)$$

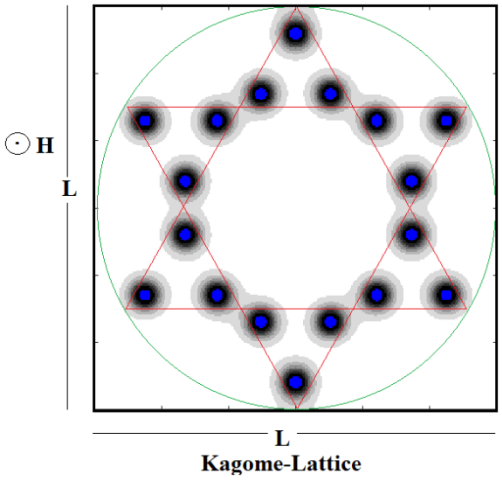

Figure 1. Layout of the studied sample: superconducting two-condensate thin square of size $L = 30\xi_{10}$ with a Kagome-lattice of circular defects of radius $r = \xi_{10}$, in presence of a perpendicular magnetic field H at $T = 0$.

Here, we will neglect the z-dependence on the order parameter in the limit of thin film $d << \xi_{10}$ [12], [13], [14], [26], [27], [28]. We will consider $\alpha_i = \alpha_{i0}(1 - T/T_{ci})$ and β_i are two phenomenological parameters, i = 1, 2 in the equations 1 and 2. We used the Josephson coupling showed in the equation 3. We express the temperature T in units of the critical temperature T_{c1}, length in units of the coherence length $\xi_{10} = \hbar/\sqrt{-2m_1\alpha_{10}}$, the order parameters in units of $\psi_{i0} = \sqrt{-\alpha_{i0}/\beta_i}$, time in units of the Ginzburg Landau characteristic time $t_{GL} = \pi\hbar/8k_B T_{c1}$, and the vector potential $\boldsymbol{A}$ is scaled by $H_{c2}\xi_{10}$, where H_{c2} is the bulk upper critical field. Although we consider $T = 0$ in our simulations, the generalized time dependent-Ginzburg-landau equations can be applied to superconductors at $T \geq 0{,}5T_c$, or equivalently, the sizes can be adjusted according to $\xi(T) = \xi(0)(1 - T/T_c)^{-0.5}$. For instance, for $T = 0{,}96T_c$, and $\xi(0) = 10nm$, we have $\xi = 50nm$ for thin Nb films. This gives $L = 600nm$. The two-condensate superconductor dynamical equations in dimensionless units, is given by [1], [7], [8], [29], [30]:

$$\frac{\partial \psi_1}{\partial t} = \varphi_1(\mathbf{r}) - |\mathbf{D}|^2\psi_1 + \gamma|\psi_2|e^{i\theta_2} \quad (4)$$

$$\frac{\partial \psi_2}{\partial t} = \varphi_2(\mathbf{r}) - \frac{m_{r2}}{\alpha_{r2}}|\mathbf{D}|^2\psi_2 + \gamma|\psi_1|e^{i\theta_1} \quad (5)$$

where $\boldsymbol{D} = i\nabla - \boldsymbol{A}$, and $\varphi i(r) = (f(\boldsymbol{r}) - |\psi i|^2)\,\psi i, i = 1{,}2$. The equation for the vector potential $\boldsymbol{A}$.

$$\frac{\partial \mathbf{A}}{\partial t} = \mathbf{J}_s - \kappa^2 \nabla \times \nabla \times \mathbf{A} \quad (6)$$

where:

$$\mathbf{J}_s = \zeta_1 \Re\mathrm{e}[\psi_1 \mathbf{D}\psi_1^*] + \zeta_2 \Re\mathrm{e}\left[\frac{\beta_{r2}}{\alpha_{r2}}\psi_2 \mathbf{D}\psi_2^*\right] \quad (7)$$

For this case, $\zeta_1 = \zeta_2$, also, and γ represents the strong of the Josephson coupling between the i and j band. The boundary conditions $\mathbf{n} \cdot \mathbf{J}_s = i\psi/b$, a superconductor-dielectric interface is simulated by $(\mathrm{b} \to \infty)$. $\mathbf{n}$ outer surface normal vector. Finally, for the coupling constants $m_{r2} = m_2 m_1^{-1} = 0.5, \beta_{r2} = \beta_2\beta_1^{-1} = 0.7, \gamma = -0.01$, $\zeta_1 = \zeta_2 = 0.01$ the Ginzburg-Landau parameter $\kappa = 1.0$ [29], [30]. For the computational mesh we use $\Delta x = \Delta y = 0.25$ and the convergence rule for the time $\Delta t \leq min(0.25\zeta^{-2}, 0.25\kappa^{-2}\zeta^{-2})$, with $\zeta^{-2} = 2/((\Delta x)^{-2} + (\Delta y)^{-2})$. The function $f(\boldsymbol{r}) = 1$ for all regions except in the Kagome lattice defects were we choose $f(\boldsymbol{r}) = 0.1$ simulating a thermal defect at lower critical temperature T_c, and, $f(\boldsymbol{r})$ incorporates the temperature dependence as $f(\boldsymbol{r}) = (T_c(\boldsymbol{r}) - T)(T_{c1} - T)^{-1}$, where T is the working temperature, T_{c1} is the nominal critical temperature of the sample and $T_c(\boldsymbol{r})$ captures the spatially nanoengineered critical temperature in the sample [24], [31].

3. Results

In the Figure 2, we plot the magnetization curve $-4\pi M$ as a magnetic field function H, and the superconducting-electron density of the dominant band $|\psi_1|^2$ (right) and its phase $\Delta\theta_1$ (left) for the ultra-stable-vortex state in the down-branch of the magnetic field at $H_2 > H > H^*$ (Inset). As we can see this curve presents the typical behaviour of a type II superconducting sample, where each jump represents the entry or exit of one or several vortices of the sample. H_2 representes the

superconducting-normal transition magnetic field and $H^* = 0.3$, the magnetic field where the ultra-stable-vortex state is destroyed. We think that this interesting state is due to the heigh of the topological coupling used betwee the bands.

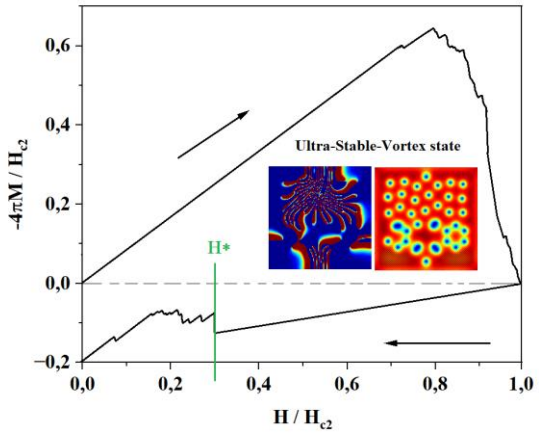

Figure 2. Magnetization curve $-4\pi M$ as a magnetic field function. (Inset) Superconducting-electron density of the dominant band $|\psi_1|^2$ and its phase $\Delta\theta_1$ for the ultra-stable-vortex state in the down-branch of the magnetic field at $H_2 > H > H^*$.

In the Figure 3 (a-d) we plot the superconducting order parameter relationet to electronic density n_s as $n_s = |\psi_1|^2$ of the dominant band, increasing the magnetic field (arrow up) for a) $H = 0.70$, $N = 0$, b) $H = 0.80$, $N = 4$, c) $H = 0.85$, $N = 16$, and d) $H = 0.89$, $N = 36$, N is the vorticity. We can observe that the vortex entry of occurs in an un-conventional way in this system. The first $N = 2$ vortices, enter through the middle region $(\pm L/2)$ in the sample, it is to be expected that the next vortices enter through the opposite sides to the sides through which the first two entered,but it does not happen like this, the entrance is always given by the same region, this is due to the nature of the two condensates of the material and its coupling between bands, as it does not happen in a conventional one-band superconductor [24]. It is important to note that due to the high of the coupling used, the configuration and size of the pinning-centers, the vortex configuration in band 2 is highly dependent on band 1 or the dominant band, therefore, in our study, we found no notable difference between these configurations and we only report results from the dominant band.

In the same way, In the Figure 4 (a-d) we plot the superconducting-electron density of the dominant band $|\psi_1|^2$, decreasing the magnetic field (arrow down) for a) $H = 0.02, N = 20$, b) $H = 0.10, N = 22$, c) $H = 0.20, N = 24$, and d) $H = 0.89, N = 40$.

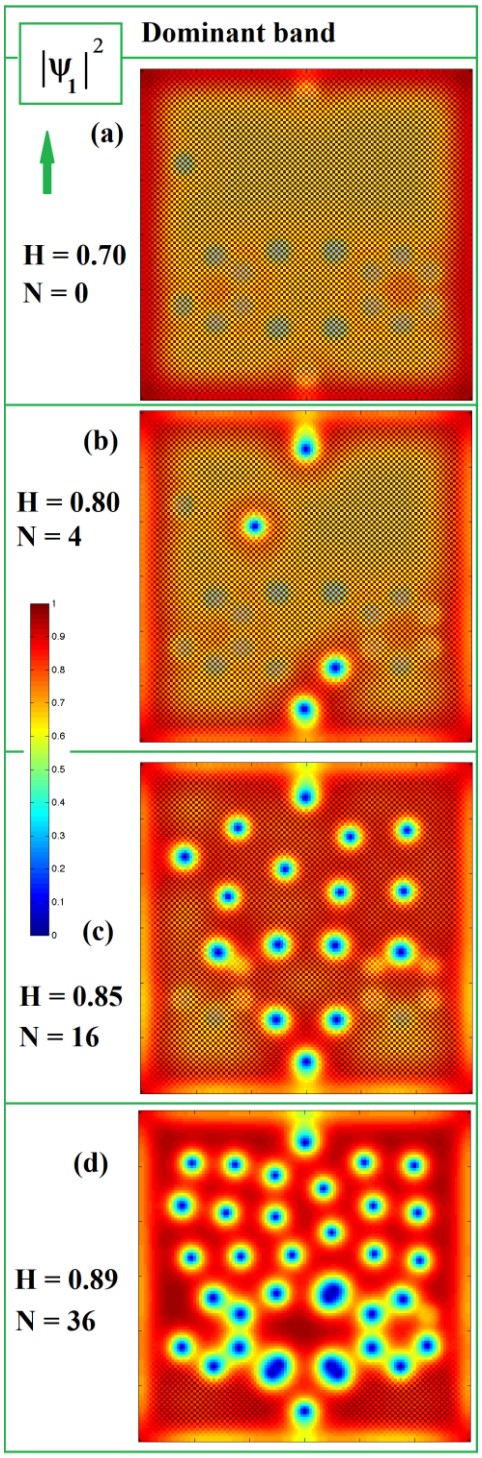

Figure 3. Superconducting-electron density of the dominant band $|\psi_1|^2$, decreasing the magnetic field (arrow down) H for a) H=0.70, N=0, b) H=0.80, N=22, c) $H = 0.20, N = 24$, and d) H=0.89, N=40, where N is the vorticity. Red (blue) regions represent a superconducting (normal) state $\psi_1 = 1(0)$.

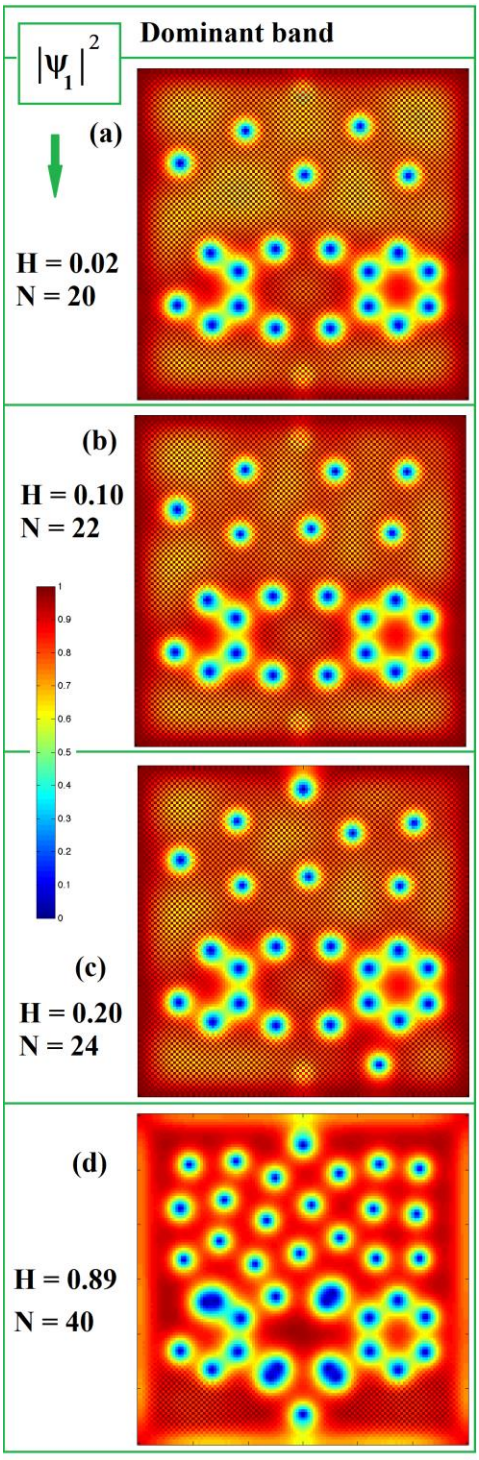

Figure 4. Superconducting-electron density of the dominant band $|\psi_1|^2$, decreasing the magnetic field (arrow down) H for a) H=0.02, N=20, b) H=0.10, N=22, c) H=0.20, N=24, and d) H=0.89, N=40, where N is the vorticity. Red (blue) regions represent a superconducting (normal) state $\psi_1 = 1(0)$.

It is interesting to note that in the down-branch of the magnetic field (decreasing H), the pinning centers play a very important role in the vortex configuration, thus, between $0.8 \lesssim H \lesssim 0.3$ we find a highly stable vortex configuration (Figure 4 (c)), remains practically unaltered in this magnetic field interval, we think that this is a very important result in practical applications, since we found a magnetic field interval for which the configuration of pinning centers allows us to have a permanent control of the voracity within the sample. For $H^* < 0.3$, the vortex exit occurs only in the upper part of the sample, keeping the vortex configuration in the lower part practically stable. In the same way, we attribute this fact to the coupling used and the size of the defect lattice Kagome structure. It is interesting to note that when the magnetic field increases in the lower left part of Figure 4, a hexagonal vortex structure is formed, which is highly stable in the sample, both when the field increases and when it decreases, when the magnetic field decreases, the expulsion of vortices is given by the regions far from these configurations. This interesting result can be attributed to the fact that the sample is of two-condensates with a coupling between the bands.

In the Figure 5 (a-b) we plot the magnetic induction B related to magnetic vectorial potential A as, $\boldsymbol{B} = \nabla \times \boldsymbol{A}$, for a dominant band, for a) H=0.80, and b) H=0.85, increasing (arrow up) and decreasing (arrow down) H. We can observe that in the superconductin state the order parameter $\psi = 1.0$ while de local magnetic induction $B = 0$ and in the regions where there are vortices $\psi = 0$ and $B = 1.0$, result completely in agreement with the already known experimental data.

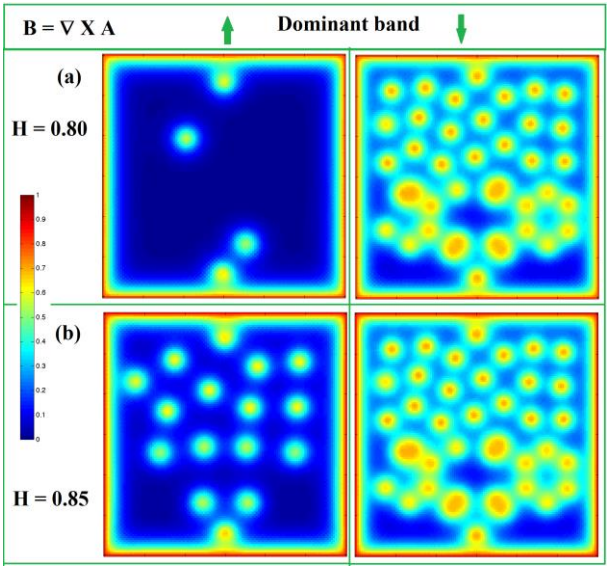

Figure 5. Magnetic induction $\boldsymbol{B} = \nabla \times \boldsymbol{A}$ for a dominant band, for a) H=0.80, and b) H=0.85, increasing (arrow up) and decreasing (arrow down) H.

Also, we can corroborate the result obtained, where we assert the existence of an ultra-stable vortex configuration, between $0.8 \lesssim H \lesssim 0.3$. We see that this vortex configuration exists in $0.8 \lesssim H \lesssim 0.85$ in the down-branch of the magnetic field, this ultra-stable-configuration does not exist in the up-branch of the magnetic field.

In the Figure 6 (a-b) we plot the phase of the order parameter of the dominant band $\Delta\theta_1$ for a) H=0.80, and b) H=0.85, increasing (arrow up) and decreasing (arrow down) H. When the Kagome-lattice of defects is placed in the sample, the square symmetry is broken and the lattice acts like a pinning center. The phase allows to determine the vortex number in a given region, by counting the phase variation in a closed path around this region. If the vorticity in this region is N, then the phase changes by $2\pi N$.

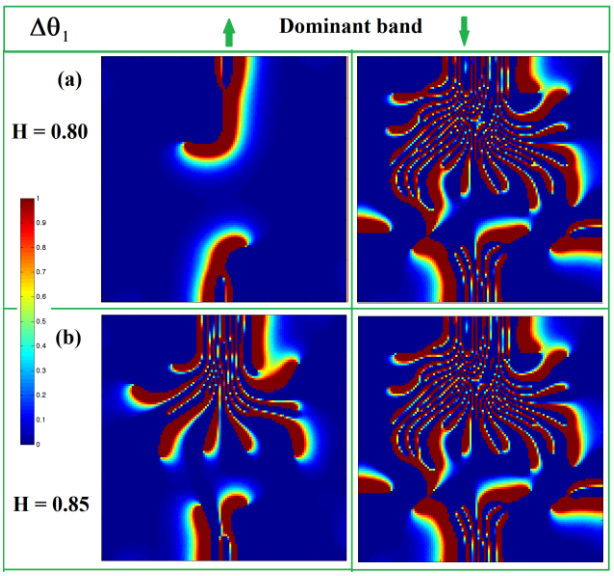

Figure 6. Phase of the order parameter of the dominant band $\Delta\theta_1$ for a) H=0.80, and b) H=0.85, increasing (arrow up) and decreasing (arrow down) H. Here blue and red regions represent values of the modulus of the order parameter (as well as $\Delta\theta_1/2\pi$), from 0 to 1.

4. Conclusions

We studied theoretically the vortex spatial distribution in a two-condensate superconducting thin square with a Kagome-lattice of topological defects. The presence of this lattice and the coupling high between the bands affects the vortex entry and the vortex configuration in the sample. We found an interesting non-conventional ultra-stable vortex configuration in the down-branch of the magnetic field, this a very important result, because we can to control de resistive state (vortex matter) in the sample by controlling the internal structure of topical defects into the sample. This non-typical behavior of the vortex-matter for a two-band sample, considering a Josephson coupling between bands, i can be explained with a non-monotonic vortex interaction, i.e, short-range repulsion and long-range attraction. Finally, we think that we did not find any difference in the vortex configurations in the bands, it is due of the chosen values of the heigh of the coupling and the size of the defects in the Kagome-lattice.

Funding acquisition

C. A. Aguirre, would like to thank the Brazilian agency CAPES, for financial support and the Ph.D, Grant number: 0.89.229.701-89.

Autor Contributions

C. A. Aguirre: Conceptualization, Formal Analysis, Writing- original draft, Writing -review & editing. P. Diaz: Conceptualization, Formal Analysis, Writing- original draft, Writing -review & editing. J. Barba-Ortega: Formal Analysis, Writing- original draft, Writing -review & editing.

Conflicts of Interest

The authors declared no potential conflicts of interest with respect to the research, authorship, and/or publication of this article.

Institutional Review Board Statement

Not applicable.

Informed Consent Statement

Not applicable.

References

[1] J. Barba-Ortega, M. R. Joya, E. Sardella, " Resistive state of a thin superconducting strip with an engineered central defect", *The European Physical Journal B*, vol. 92, no. 143, 2019, doi: https://doi.org/10.1140/epjb/e2019-100082-y

[2] G. J. Kimmel, A. Glatz, V. M. Vinokur, I. A. Sadovskyy, "Edge effect pinning in mesoscopic superconducting strips with non-uniform distribution of defects," *Sci. Reports*,vol. 9, no. 1, 2019, doi: https://doi.org/10.1038/s41598-018-36285-4

[3] V. V. Moshchalkov, L. Gielen, C. Strunk, R. Jonckheere, X. Qiu, C. Van Haesendonck and Y. Bruynseraede, "Effect of sample topology on the critical fields of mesoscopic superconductors," *Nature* vol. 373, 1995, doi: https://doi.org/10.1038/373319a0

[4] C. Aguirre, M. R. Joya, J. Barba-Ortega, "Released power in a vortex-antivortex pairs annihilation process," *Revista UIS Ingenierias*, vol. 20, no. 1, 2021, doi: https://doi.org/10.18273/revuin.v20n1-2021014

[5] C. Aguirre, M. R. Joya, J. Barba-Ortega, "Dimer structure as topological pinning center in a superconducting sample," *Revista UIS Ingenierias*, vol. 20, no. 1, 2020, doi: https://doi.org/10.18273/revuin.v19n1-2020011

[6] J. Carlstrom, E. Babaev, M. Speight, "Type-1.5 superconductivity in multiband systems: Effects of interband couplings," *Phys. Rev. B.*, vol. 83, 2011, doi: https://doi.org/10.1103/PhysRevB.83.174509

[7] C. Aguirre, J. Faundez, J. Barba-Ortega, "Vortex state in a superconducting mesoscopic irregular octagon," *Mod. Phys. Lett. B.*, vol. 36, 10, 2022, doi: https://doi.org/10.1142/S0217984922500294

[8] C. Aguirre, M. R. Joya, J.Barba-Ortega, "Vortex state in a two-condensate superconducting film considering a topological coupling, " *Mod. Phys. Lett. B*, vol 37, no. 38, 2023, doi: https://doi.org/10.1142/S021798492350001X

[9] C. Aguirre, A. de Arruda, J. Faundez, J. Barba-Ortega, "ZFC process in 2+1 and 3+1 multi-band superconductor," *Physica B: Condensed Matter*, vol. 615, 2021, doi: https://doi.org/10.1016/j.physb.2021.413032

[10] J. Tindall, F. Schlawin, M. Buzzi, D. Nicoletti, J. R. Coulthard, H. Gao, A. Cavalleri, M. A. Sentef, D. Jaksch, "Dynamical Order and Superconductivity in a Frustrated Many-Body System," *Phys. Rev. Lett*., vol. 125, 2020, doi: https://doi.org/10.1103/PhysRevLett.125.137001

[11] E. F. Galindez, J. A. Rojas, D. Sachez, D. A. Landinez, J. Roa, "Propiedades ópticas, eléctricas, estructurales y morfológicas de arcilla mineral KAl4Si2O12/Mg3Si2O9/Fe2O3 de la región montañosa de Machado, Tarairá, Colombia" *Revista Ciencia en Desarrollo*, vol. 13, no. 1, pp. 43-55, 2022, doi: https://doi.org/10.19053/01217488.v13.n1.2022.12884

[12] W. D. Gropp, H. G. Kaper, G. K. Leaf, D. M. Levine, M. Palumbo, V. M. Vinokur, "Numerical simulation of vortex dynamics in type-ii superconductors," *J. Comput. Phys*., vol. 123, no. 2, 1996, doi: https://doi.org/10.1006/jcph.1996.0022

[13] G. Buscaglia, C. Bolech, C. Lopez, *Connectivity and Superconductivity*. Heidelberg: Springer, 2000, doi: https://doi.org/10.1007/3-540-44532-3

[14] P. G. de Gennes, *Superconductivity in Metals and Alloys*, Westview Pres, 1989. [Online]. Available: https://library.navoiy-uni.uz/files/gennes%20p.d.,%20pincus%20p.a.%20-%20superconductivity%20of%20metals%20and%20alloys%20(1999)(274s).pdf

[15] Z. P. Yin, K. Haule, G. Kotliar, "Fractional power-law behavior and its origin in iron-chalcogenide and ruthenate superconductors: Insights from first-principles calculations," *Phys. Rev. B*, vol. 86, 2012, doi: https://doi.org/10.1103/PhysRevB.86.195141

[16] J. Clepkens, A. W. Lindquist, X. Liu, H. Kee, "Higher angular momentum pairings in interorbital shadowed-triplet superconductors: Application to Sr2RuO4," *Phys. Rev. B.*, vol. 104, 2021, doi: https://doi.org/10.1103/PhysRevB.104.104512

[17] S. Chaudhar, Shama, J. Singh, A. Consiglio, D. Di Sante, R. Thomale, Y. Singh, "Role of electronic correlations in the kagome-lattice superconductor LaRh3B2," *Phys. Rev. B.*, vol. 107, 2023, doi: https://doi.org/10.1103/PhysRevB.107.085103

[18] M. Shi, F. Yu, Y. Yang, F. Meng, B. Lei, Y. Luo, Z. Sun, J. He, R. Wang, Z. Jiang, Z. Liu, D. Shen, T. Wu, Z. Wang, Z. Xiang, J. Ying and X. Chen, "A new class of bilayer kagome lattice compounds with Dirac nodal lines and pressure-induced superconductivity," *Nature Communicatios*, vol. 13, 2022, doi: https://doi.org/10.1038/s41467-022-30442-0

[19] H. Jiang, M. Liu, S. Yu, "Impact of the orbital current order on the superconducting properties of the kagome superconductors, " *Phys. Rev. B.*, vol. 107, 2023, doi: https://doi.org/10.1103/PhysRevB.107.064506

[20] F. Du, R. Li, S. Luo, Y. Gong, L. Yanchun, J. Sheng, R. B. ˙Ortiz, Y. Liu, X. Xu, S. D. Wilson, C. Cao, Y. Song, H. Yuan, "Superconductivity modulated by structural phase transitions in pressurized vanadium-based kagome metals," *Phys. Rev. B.*, vol. 106, 2022, doi: https://doi.org/10.1103/PhysRevB.106.024516

[21] S. Gazit, M. Randeria, A. Vishwanath, "Emergent Dirac fermions and broken symmetries in confined and deconfined phases of Z2 gauge theories," *Nature Physics*, vol. 13, pp. 484-490, 2017, doi: https://doi.org/10.1038/nphys4028

[22] T. Neupert, M. Denner, J. Yin, R. Thomale M. Zahid Hasan, "Charge order and superconductivity in kagome materials," *Nature Physics*,vol. 18, 2022, doi: https://doi.org/10.1038/s41567-021-01404-y

[23] K. Jiang, T. Wu, J. Yin, Z. Wang, M. Hasan, S. Wilson, X. Chen J. Hu, "Kagome superconductors AV3Sb5 (A = K, Rb, Cs)," *National Science Review*, vol. 10, 2023, doi: https://doi.org/10.1093/nsr/nwac199

[24] J. S. Leon. M. R. Joya and J. Barba-Ortega, "Kagome–Honeycomb structure produced using a wave laser in a conventional superconductor," *Optik-International Journal for Light and Electron Optics*, vol. 172, pp. 311-316, 2018, doi: https://doi.org/10.1016/j.ijleo.2018.07.036

[25] R. Lou, A. Fedorov, Q. Yin, A. Kuibarov, Z. Tu, C. Gong, E. F. Schwier, B. Buchner, H. Lei, S. Borisenko, "Charge-Density-Wave-Induced Peak-Dip-Hump Structure and the Multiband Superconductivity in a Kagome Superconductor CsV3Sb5," *Phys. Rev. Lett.*, vol. 128, 2022, doi: https://doi.org/10.1103/PhysRevLett.128.036402

[26] S. J. Chapman, Q. Du, M. S. Gunzburger, Z. Angnew, "A model for variable thickness superconducting thin films," *Math. Phys*., vol. 47, 1996, doi: https://doi.org/10.1007/BF00916647

[27] Q. Du. M. D. Gunzburger, J. S. Peterson, "Computational simulation of type-II superconductivity including pinning phenomena," *Phys. Rev. B.*, vol. 51, 1995, doi: https://doi.org/10.1103/PhysRevB.51.16194

[28] Q. Du, M.D. Gunzburger, "A model for superconducting thin films having variable thickness," *Physica D: Nonlinear Phenomena*, vol. 69, 1993, doi: https://doi.org/10.1016/0167-2789(93)90089-J

[29]V. S. Souto E. C. S. Duarte, E. Sardella, R. Zadorosny, "Kinematic vortices induced by defects in gapless superconductors," *Phys. Lett. A.*, vol. 419, 2021, doi: https://doi.org/10.1016/j.physleta.2021.127742

[30] A. Benfenati, A. Samoilenka, E. Babaev, "Boundary effects in two-band superconductors," *Phys. Rev. B.*, vol. 103, 2021, doi: https://doi.org/10.1103/PhysRevB.103.144512

[31] A. Crassous, R. Bernard, S. Fusil, K. Bouzehouane, D. Le Bourdais, S. Enouz-Vedrenne, J. Briatico, M. Bibes, A. Barthelemy, J. E. Villegas, "Nanoscale Electrostatic Manipulation of Magnetic Flux Quanta in Ferroelectric/Superconductor BiFeO3/YBa2Cu3O7−δ Heterostructures," *Phys. Rev. Lett.*, vol. 107, 2011, doi: https://doi.org/10.1103/PhysRevLett.107.247002